

Electronic Supporting Information

Surface-initiated mechano-ATRP as a convenient tool for tuning of bidisperse magnetorheological suspensions toward extreme kinetic stability

*Martin Cvek,^{*a} Jozef Kollar,^b Miroslav Mrlik,^a Milan Masar,^a Pavol Suly,^a Michal Urbanek^a
and Jaroslav Mosnacek^{*b,c}*

^a Centre of Polymer Systems, University Institute, Tomas Bata University in Zlín, Trida T.

Bati 5678, 760 01 Zlín, Czech Republic

^b Polymer Institute, Slovak Academy of Sciences, Dubravská cesta 9, 845 41 Bratislava,
Slovakia

^c Centre for Advanced Materials Application, Slovak Academy of Sciences, Dubravská
cesta 9, 845 11 Bratislava, Slovakia

*Authors to whom correspondence should be addressed: cvek@utb.cz and

jaroslav.mosnacek@savba.sk

Keywords: magnetorheology; ATRP; synthesis; polymer; ultrasound; nanoparticles

When devising the coating procedure, the SSA values of the intermediate substrates (the neat NPs, NPs-NH₂ and NPs-Br) were gauged to determine what amounts of the coating agents would be suitable (see the main text). Figure S1 details the corresponding nitrogen adsorption/desorption isotherms, the curves of which were classified as reversible type II according to a IUPAC Technical Report.¹ The isotherm of the neat NPs exhibited low hysteresis, indicating weak interactions between the particles and adsorbed molecules

(Fig. S1a). This sample initially showed an SSA value of $110 \text{ m}^2/\text{g}$ and a total pore volume of $0.38 \text{ cm}^3/\text{g}$, decreasing to $39 \text{ m}^2/\text{g}$ and $0.30 \text{ cm}^3/\text{g}$ after silanization, respectively; another drop to $36 \text{ m}^2/\text{g}$ and $0.27 \text{ cm}^3/\text{g}$ occurred upon BiBB bonding. The evolution of surface characteristics confirmed the efficiency of the coating reactions, and confirmation of the success of the coating procedure by analytical methods is given in the main text. For the comparison purposes, the isotherm for the CI particles was collected showing a certain hysteresis that stems from the adsorbent-adsorptive interactions. Their SSA value equalled $0.23 \text{ m}^2/\text{g}$, which is much smaller value compared to that of nano-additives.

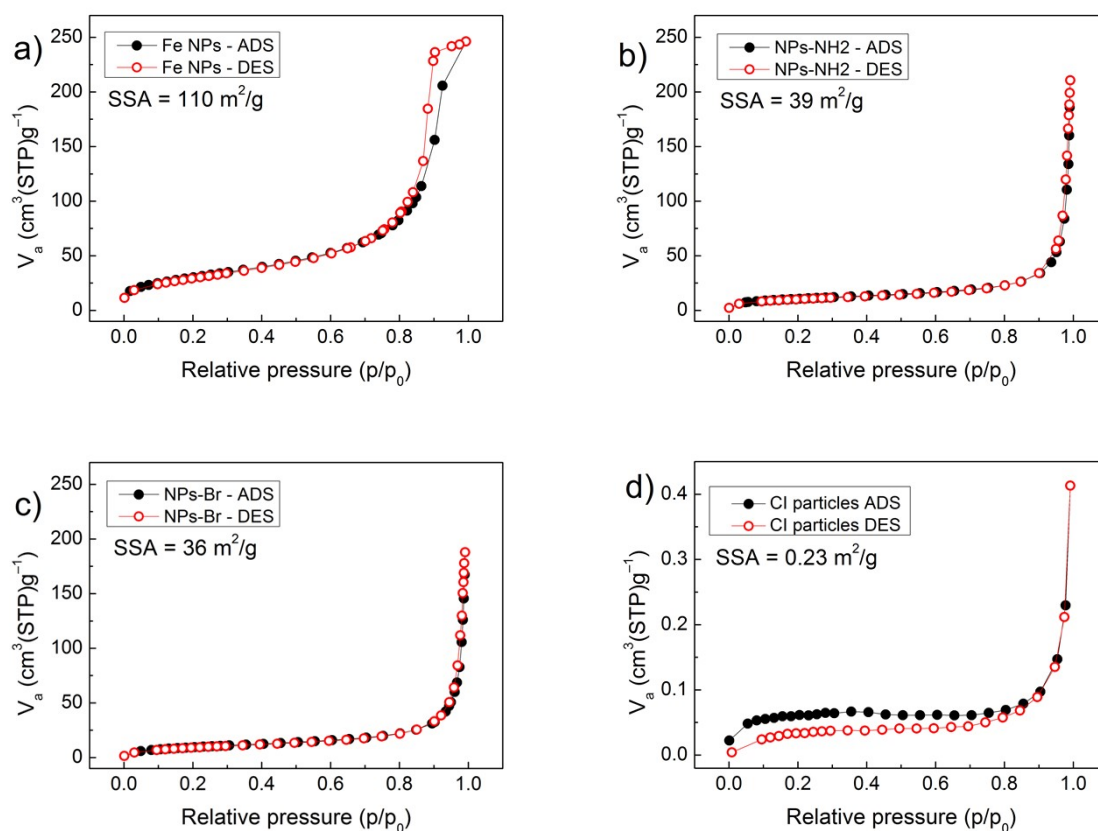


Figure S1: Nitrogen adsorption/desorption (*solid / open symbols*) isotherms for (a) the neat NPs, (b) NPs-NH₂, (c) NPs-Br nano-species and (d) the CI particles (SL grade).

The custom-produced ZnO was applied as a piezoelectric transducer to mediate the mechano-ATRP process. The morphology of the powder was investigated by SEM, as displayed in Figure S2a. As seen therein, the ZnO nanoparticles were joined together by small bridges, forming well-defined building blocks at a microscale level (hereafter referred to as micro-ZnO), which ultimately led to a relatively low SSA value of micro-ZnO. Looking closer at the structure, it was distinguished that the blocks were composed of spherical primary NPs. Figure S2b shows the EDX spectrum with evidence of elemental composition, the peaks in it relating solely to the elements of Zn and O and indicating the material was free of impurities. XRD analysis was performed to further examine structural integrity, as displayed in Fig. S2c. The average crystallite size, d , of the micro-ZnO calculated from (101) the width of the diffraction line equalled ca 14 nm. The Scherrer equation, $d = K\lambda/\beta\cos\theta$, was applied for the calculation, thereby approximating the spherical crystallite shape (the shape factor K of 0.9) since no preferential orientation had been observed. The wavelength of the radiation was discerned as $\lambda(\text{CoK}\alpha_{1,2}) = 0.179$ nm, wherein the angle θ constituted a half of the value 2θ for the corresponding diffraction line, and β was the full width at a half-maximum intensity of a peak observed at a mean scattering angle of 2θ . The XRD data also evidenced the successful transformation of the precursor into the micro-ZnO. The initial material, i.e. $\text{ZnC}_2\text{O}_4 \times 2\text{H}_2\text{O}$, showed several diffraction lines that matched with standard PDF Card No.: 00-025-1029, corresponding with the monoclinic-phase structure. After the annealing procedure, the micro-ZnO exhibited diffraction peaks pertaining to the crystallographic planes (100), (002), (101), (102), (110), (103), (200), (112) and (201) typical for hexagonal-phase ZnO.² The diffraction lines detected were in good agreement with standard PDF Card No. 01-080-0075. Moreover, the sharpness of the diffraction lines implied a high degree of crystallinity. It is noteworthy that the fabrication route of precipitation and annealing can be scaled up to produce a large amount of high purity piezoelectric micro-ZnO transducers.

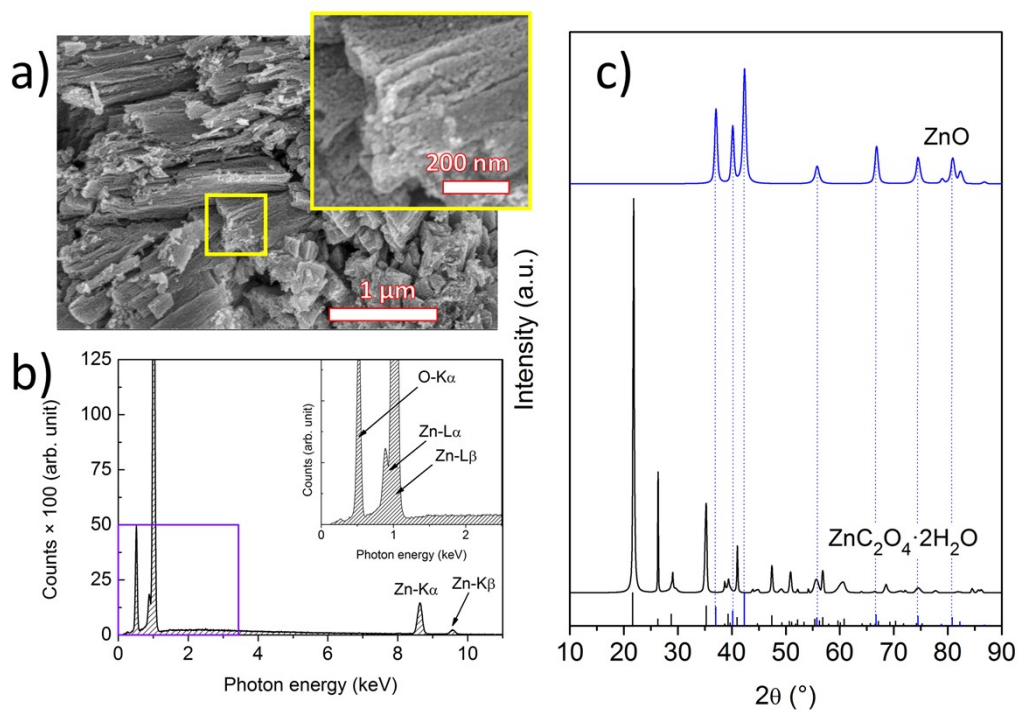


Figure S2: SEM micrographs of (a) the magnified view (*inset*), EDX spectrum (b) and XRD patterns (c) of the custom-produced micro-ZnO particles.

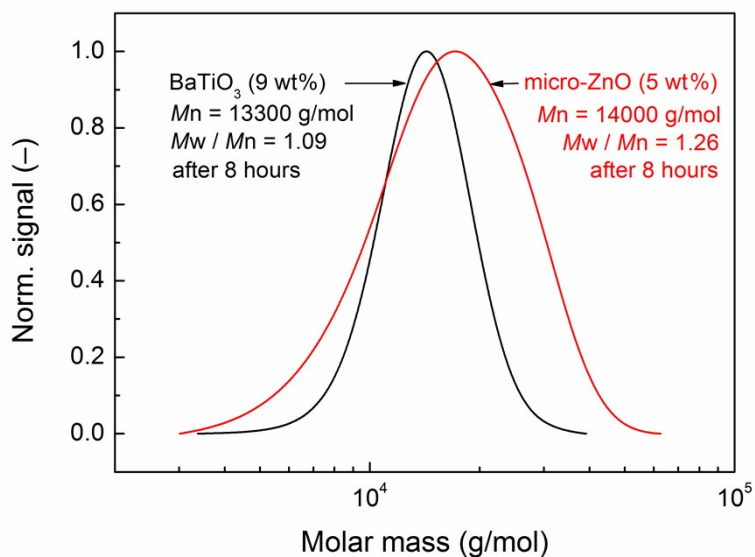


Figure S3: GPC traces of PMA synthesized via mechano-ATRP mediated using cubic-phase BaTiO $_3$ and hexagonal micro-ZnO (without the magnetic NPs-Br in the reaction systems).

Declaration of interest: There are no conflicts to declare.

Acknowledgements

The authors M.C., M.M. (Milan Masar), P.S. and M.U. gratefully acknowledge the project DKRVO (RP/CPS/2020/006) supported by the Ministry of Education, Youth and Sports of the Czech Republic. This research was also supported by the National Scholarship Programme of the Slovak Republic, funded by the Ministry of Education, Science, Research and Sport of the Slovak Republic (project ID: 27926). The research reported herein was performed under the framework of a project entitled the “Building-up Centre for advanced materials application of the Slovak Academy of Sciences”, ITMS project code 313021T081, supported by the Integrated Infrastructure Operational Programme funded by the ERDF. The author J.M. is grateful for financial support for the projects VEGA 2/0129/19 and APVV-19-0338

References

- (1) Thommes, M.; Kaneko, K.; Neimark, A. V.; Olivier, J. P.; Rodriguez-Reinoso, F.; Rouquerol, J.; Sing, K. S. W. Physisorption of gases, with special reference to the evaluation of surface area and pore size distribution (IUPAC Technical Report). *Pure Appl. Chem.*, 2015, **87**, 1051-1069, DOI: 10.1515/pac-2014-1117.
- (2) Soares, V. A.; Xavier, M. J. S.; Rodrigues, E. S.; de Oliveira, C. A.; Farias, P. M. A.; Stingl, A.; Ferreira, N. S.; Silva, M. S. Green synthesis of ZnO nanoparticles using whey as an effective chelating agent. *Mater. Lett.*, 2020, **259**, 126853, DOI: 10.1016/j.matlet.2019.126853.